Constrained Inverse Dynamics and Feet-Terrain Interaction Modelling of a Staircase Climbing Hexapod Robot

Abhijit Mahapatra, Shibendu Shekhar Roy, Dilip Kumar Pratihar

Abstract

In the present study, the constrained inverse dynamics model using Newton-Euler approach has been developed for a realistic hexapod robot. For a more realistic locomotion analysis, oblique impact of feet-tip with the terrain is considered, which is governed by a compliant impact force model. It is assumed that the prescribed motion of the model is fully known and consistent with the kinematic constraints of the realistic model. The kinematic motion parameters (displacement, velocity and acceleration) obtained from the inverse kinematic analysis with specified path and gait planning for straight-forward motion in varying terrains are substituted in the inverse dynamic model to determine the dynamic motion parameters that are responsible to generate the prescribed motion trajectories. The solution is not unique due to the redundant set of forces/ moments and/or constraints used. Therefore, the contact force distribution in the feet during interaction with the terrain is considered to be a constrained optimization problem, where minimizing the sum of the squares of joint torques of the system has been considered as the objective function along with some linear equality and inequality constraints. The paper also investigates the optimal feet forces' distributions under body forces, joint torques, total power consumption etc. without any external disturbance during the robot's locomotion on a staircase.

Keywords: Hexapod Robot, Straight-Forward Motion, Staircase Climbing, Inverse Dynamics, Feet-Terrain Interaction, Optimization, and Power Consumption

1 Introduction

The performance of a robotic system to complete any assigned task depends on its physical contact with the surroundings. Some examples are like the foot of a legged robot interacting with the terrain or colliding with obstacles during locomotion [1], robotic finger grasping an object [2], manipulators handling or colliding with foreign objects during operation in an unknown environment [3] etc. Therefore, modelling of contact including collision or impact is an important part of dynamic simulation of a robotic system. Most of the studies on contact simulation carried out by the previous

Abhijit Mahapatra
Virtual Prototyping & Immersive Visualization Lab, CSIR-Central Mechanical Engineering Research Institute, Durgapur 713209, India. Email:abhi_mahapatra@yahoo.co.in

Shibendu Shekhar Roy (Corresponding author)
Department of Mechanical Engineering, National Institute of Technology, Durgapur 713209, India.
Email:ssroy99@yahoo.com

Dilip Kumar Pratihar
Department of Mechanical Engineering, Indian Institute of Technology, Kharagpur 721302, India.
Email:dkpra@mech.iitkgp.ernet.in

researchers worldwide on robotic systems assumed the contacting point as perfectly rigid [4-6]. But, it is to be remembered that for frictional contact surface with coulomb's friction model or otherwise, the idea of objects as rigid bodies is not a realistic assumption. In few cases, it might lead to infeasible solutions to the problems. So, a few researchers also included compliance between the contacting bodies to avoid such problems arising from rigid body assumptions [1,7-9]. Simplified models of objects were studied to handle impacts, sustained contact under load and transitions conditions (to and from contact). The present study focuses on modeling the compliance between the leg tip and terrain at the region of contact for legged robots like the hexapod configuration. An attempt is made to develop the compliant contact force model with oblique impact of feet-tip with terrain for a realistic hexapod robotic system, which is far more a complex configuration. The normal component of the contact force model is analogous to the impact-based contact model used in MSC.ADAMS®, which again is the non-linear Hunt-Crossley model [10] subjected to some modifications. Also, it is to be noted that the tangential compliance between the leg tip and terrain is assumed to be negligible in the contact region, which is a case of no-slip condition.

Further, it is necessary to develop a constrained inverse dynamics model to tackle the dynamics of the rigid bodies of the system [11, 12]. But, the models were simplified due to the complexities with respect to both the mechanical structure (a body and jointed legs) and locomotion planning (that is, path and gait planning) on varying terrains. Various approaches (Newton-Euler, Lagrange-Euler etc.) were used to study the dynamics of the systems, but the models neglected the coupling effects and non-linearity in the dynamics of the swing legs on the support legs and the trunk body. It is to be noted that the locomotion of a legged robot on rough and uneven terrain is a coupled dynamical problem, where the inertia effects of swing legs on support legs is an issue. The present study deals with such coupling effects during the robot's locomotion. This makes the constrained inverse dynamic model more realistic and is illustrated with the help of a robot moving on an uneven terrain like climbing a staircase. Such a comprehensive dynamic model is crucial in the design, energy efficiency and control of legged robots.

The solution to such type of problems is not unique due to the redundant set of forces/ moments and/or constraints used. Therefore, the contact force distribution in the feet during interaction with the terrain is considered to be a constrained optimization problem. The optimization methods implemented by various researchers to obtain the feet forces and study the dynamics of the legged robots include linear programming [13], quadratic programming [14, 15], pseudo inverse [16] or additional constraint equation to create a determinate set [17]. In the present study, a naturalistic objective function imposed is the minimization of the sum of squares of the joint torques to determine contact foot-force distribution, joint torques and total power consumption of the robotic system. In section 2 of this paper, the constrained rigid body dynamics model of a hexapod robotic system is presented. This is followed by the description of a non-linear contact force model with impact during foot-terrain interaction of the robot for a deformable foot (hard) versus hard (little deformation) terrain in Section 3. Section 4 describes the quadratic optimization methodology. Lastly, in Section 5 an illustrative example of foot contact with the terrain for a staircase climbing robot demonstrates the ability of the model to simulate feet forces in a hexapod robot during impact, support and lift-off.

2 Constrained Rigid Body Dynamics of the System

In the present study, a realistic 3D hexapod, with the configuration shown in Fig. (1), climbing up a staircase is considered. The hexapod consists of a trunk body and six legs. Each leg consists of three revolute joints, which are independently controlled by three actuators. Therefore, the hexapod can be considered as a robotic system having twenty four degrees of freedom (six DOF of the body and eighteen degree of freedom of all the legs taken together). The system has two global reference frames: 1) Static Global reference frame $\boldsymbol{G}_0$, 2) Dynamic Global reference frame $\boldsymbol{G}$ with respect to XYZ coordinate system. The frames are chosen such that $\boldsymbol{G}$ is the working frame of reference and $\boldsymbol{G}_0$ is fixed frame of reference, which defines the topography (slope, elevation etc.). In the present problem both the frames are parallel and coincides at origin **O.** Further, the trunk body has a body fixed reference frame $\boldsymbol{L}_0$ with origin at $\mathbf{P}_0$. All the bodies in the system are assumed rigid with the joint variables of each leg as θ_{i1}-β_{i2}-β_{i3} corresponding to local axes configuration. Also, the orientation vectors of Bryant angles are: 1) $\boldsymbol{\eta}_G = [\alpha_G \ \beta_G \ \theta_G]^T$ between $\boldsymbol{G}_0$ and $\boldsymbol{G}$ and 2) $\boldsymbol{\eta}_0 = [\alpha_0 \ \beta_0 \ \theta_0]^T$ between $\boldsymbol{G}$ and $\boldsymbol{L}_0$. Therefore, the vectors of Cartesian coordinates of $\mathbf{P_0}$ with respect to $\boldsymbol{G}$ are represented by $\mathbf{p}_0^G = (\mathbf{r}_{P_0O}^G, \boldsymbol{\eta}_0) \in \mathbb{R}^6$ where $\mathbf{r}_{P_0O}^G = [x_{P_0O}^G \quad y_{P_0O}^G \quad z_{P_0O}^G]^T$.

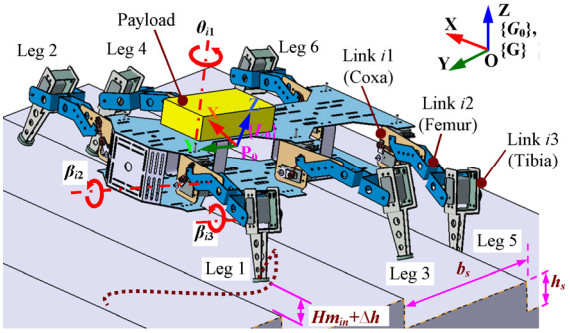

Figure 1: CAD Model of a realistic hexapod climbing up the staircase

Inverse kinematic analysis of the robotic system is carried out for a predefined three-dimensional (3D) trunk body motion, swing leg trajectory planning of the feet-tip as well as gait planning with straight-forward motion in varying terrains to calculate the angular displacement of the various joints (i=1 to 6, j=1 to 3) and finally the kinematic motion parameters like velocity, acceleration, aggregate center of mass etc. The essential robot model parameters and the locomotion parameters are as listed in Table 1. The parameters are subsequently transformed from reference frame $\boldsymbol{G}$ to frame $\boldsymbol{G}_0$ (refer to [18] for details). Kinematic analysis of the system is followed by inverse dynamic analysis to compute some of the important parameters like optimal distribution of feet forces, joint torques, power consumption etc. of the system. The constrained inverse dynamic model of the system is developed using Newton-Euler approach. The implicit constrained dynamic equation of the robotic system is given by the expression:

$$\mathbf{M(p)}.\ \dot{\mathbf{v}} = {}^c\mathbf{f} + \mathbf{f}\,(\mathbf{p}, \mathbf{v}) + \mathbf{q}_{GC}\,(\mathbf{p}, \mathbf{v}) \in \mathbb{R}^{114} \qquad (1)$$

where $\mathbf{M(p)} \in \mathbb{R}^{114,114}$ is the combined mass matrix of the robotic system; $\mathbf{v}$, $\dot{\mathbf{v}} \in \mathbb{R}^{24}$ are the velocity and acceleration vector of the system in cartesian space; ${}^c\mathbf{f}$

$\in \mathbb{R}^{114}$ being the vector of constant reaction forces and torques of the joints associated with system coordinates; $\mathbf{f(p, v)} \in \mathbb{R}^{114}$ is the vector of both known and unknown applied forces and torques; $\mathbf{q}_{GC}\mathbf{(p, v)} \in \mathbb{R}^{114}$ is the vector of centrifugal forces and gyroscopic terms.

Table 1: System Parameters of the Robot

Robot model parameters						***Locomotion Parameters***		***Foot-Ground Parameters***	
Para-meters	***Values***					***Para-meters***	***Values***	***Para-meters***	***Values***
(i=1 to 6)	Trunk body	Pay-load	Link *i1*	Link *i2*	Link *i3*	Hm_{in}	0.07m	e	2.2
Mass (Kg)	0.65	4.244	0.150	0.041	0.110	Δh	0.002m	K	1e+5N/m
I_{xx}	1.66E-2	9E-3	7.1E-5	2.0 E-5	9.8E-5	s_0	0.125m	C_{max}	10N-s/m
I_{yy}	2.52E-3	3E-3	10.8E-5	8.7 E-5	8.7E-5	v_{yz}	0.1m/s	p	0.01mm
I_{zz}	1.69E-2	11E-3	5.7E-5	10.0 E-5	2.1E-5	h_s	0.05m	μ_i	0.3
Length(m)	0.495	0.150	0.085	0.120	0.100	b_s	0.25m		

Joint offsets: d_{i1}=0.008m, d_{i2}=0.018m; d_{i3}=0.02m; Hm_{in} : maximum terrain height (on the path of swing); Δh: swing height over and above the maximum terrain height,; s_0= stroke of trunk body; v_{xz}: maximum translational velocity of the trunk body along the fixed slope of the staircase with respect to frame $\boldsymbol{G}$; h_s: height of each staircase; b_s: width of the each staircase; I_{xx} , I_{yy} and I_{zz} : mass moment of inertia values of the individual components (Kg-m^2) along their respective axes; Material density (Aluminium)=2740 Kg/m^3, n: duty cycle, i: leg number, e: force exponent (mostly material property, e>1 for non-linear spring); K: contact stiffness which is based on both material properties (young's modulus and poisson's ratio) and geometrical properties (radius of curvature), C_{max}: maximum damping; p: boundary penetration at which full damping is applied (reasonable, $p < z_1$), μ_i: coefficient of static friction in leg i.

The implicit constraint dynamic Eq. (1) is expressed in complete cartesian coordinates (**p**), which is often undesirable, since handling of the large number of equations is cumbersome and computationally intensive. Therefore, the kinematic motion parameters in cartesian space are transformed by kinematic transformation to the joint space in terms of generalized coordinates (**q**), where $\mathbf{q} \in [\mathbf{r}^{G}_{\hat{0}O}, \boldsymbol{\eta}_0, \theta_{11}, \beta_{12}, \beta_{13}, \theta_{21}, \beta_{22}, \beta_{23}, \theta_{31}, \beta_{32}, \beta_{33}, \theta_{41}, \beta_{42}, \beta_{43}, \theta_{51}, \beta_{52}, \beta_{53}, \theta_{61}, \beta_{62}, \beta_{63}]^{\mathrm{T}} \in \mathbb{R}^{24}$ such that

$$\mathbf{v} = \mathbf{J}\mathbf{u} \tag{2}$$

The final form of transformation of the dynamic model in the joint space is given by the following relation:

$$\mathbf{D(q)}\dot{\mathbf{u}} + \mathbf{C(q,\dot{q})} = \boldsymbol{\tau} \in \mathbb{R}^{24} \tag{3}$$

where,

$$\mathbf{D(q)} = \mathbf{J}^T\mathbf{M(p)}\,\mathbf{J} \in \mathbb{R}^{24\times 24} \tag{4}$$

$$\mathbf{C(q,\dot{q})} = \mathbf{J}^T\mathbf{M(p)}\dot{\mathbf{J}}\mathbf{u} \in \mathbb{R}^{24}, \tag{5}$$

$$\boldsymbol{\tau} = \mathbf{J}^T[\,\mathbf{f(p, v)} + \mathbf{q}_{GC}\mathbf{(p, v)}] \in \mathbb{R}^{24}, \tag{6}$$

Here $\mathbf{u}$ and $\dot{\mathbf{u}} \in \mathbb{R}^{24}$ are the velocity and acceleration vector of the system in joint space; $\mathbf{J} \in \mathbb{R}^{114,24}$ is the Jacobian matrix of the system in terms of generalized coordinates (**q**) related to ground reaction forces and coupled joint torques; **D(q)** is the coupled mass and inertia matrix of the robotic system in terms of generalized

coordinates; $\boldsymbol{\tau}$ is the vector of ground reaction forces ($\mathbf{F}_i$) and coupled joint torques ($\mathbf{M}_i$) i= 1 to 6. Further, the ground reaction force $\mathbf{F}_i$ at the foot of leg i with respect to $\boldsymbol{G}_0$ is denoted by vector $[F_{ix}\ F_{iy}\ F_{iz}]$ and the vector of coupled joint torques $\mathbf{M}_i$ of leg i is denoted by $[M_{i1}\ M_{i2}\ M_{i3}]^T$. Overall, twenty four number of equations are obtained in terms of ground reaction forces and coupled joint torques by substituting the necessary input values in (3).

3 Non-Linear Contact Model with Impact Response

To simplify the dynamic analysis, it is assumed that both the feet and terrain are rigid except for an infinitesimally small region surrounding the contact point, where compliance between the contacting bodies is included. The contact point is assumed to be governed by a visco-elastic model. For oblique impact between the feet-tip and terrain, the impact force **F** (refer to Fig. (2)) is composed of two components (normal and tangential direction), that is, (i) compliant normal impact force $\mathbf{F}_v$ and (ii) compliant horizontal impact force $\mathbf{F}_h$.

In the present study, the normal force model is analogous to the impact-based contact model used in MSC.ADAMS® and is basically the non-linear Hunt-Crossley model [10] subjected to some modifications. The force $\mathbf{F}_v$ for a deformable foot (hard) and hard (little deformation) terrain is governed by an impact function that depends mainly on the foot's deformation, its velocity, contact stiffness, damping etc. Hence, the normal impact force is given by,

$$\mathbf{F}_v = \begin{cases} 0 & \left.\right\} z > z_1 \\ K(z_1 - z)^e - C_{\max}.\dot{z}.STEP(z, z_1 - p, 1, z_1, 0) & \left.\right\} z \le z_1 \end{cases} \tag{7}$$

where the step function is governed by a cubic polynomial such that,

$$\text{STEP}\ (z,\ z_1\text{-}p,\ 1,\ z_1,\ 0) \equiv \left(1 - \bar{a}.\Delta_z^2\left(3 - 2\Delta_z\right)\right). \tag{8}$$

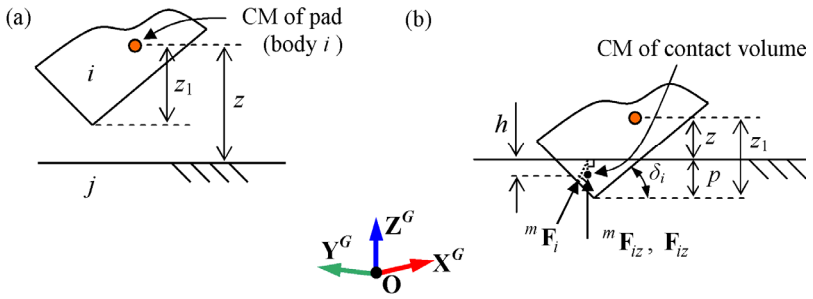

Figure 2: Foot-terrain model (a) before impact (b) after impact [h is the distance between the center of mass (CM) of the portion of the pad in contact and the ground; F_{iz} is the normal foot reaction force]

Here, $\bar{a} = 1 - 0 = 1$; $\Delta_z = \left(z - z_1 + p\right)/p$; z is the distance function, z_1 is the trigger distance; $\dot{z}$ is the derivative of z to impact; K and $C_{\max}$ are as described in the Table 1. Further, it is assumed that tangential compliance of the leg tip and the terrain is negligible in the contact region, which is a case of no-slip condition. It can also be seen that when $z \le z_1$, the impact function activates, that is, when the distance between the two objects is smaller than the free length of z (refer to Fig. (2)). Subsequently, the force becomes non-zero and consists of two parts: an exponential

spring force and a damping force that follows a step function as mentioned above. It should be noted that both the forces are strictly positive, since the calculated normal force opposes the compression that occurs during penetration.

4 Optimization Criteria for Optimal Distribution of Joint Torques

The solution to the problem is to be obtained by optimization through quadratic programming, that is, minimizing the sum of squares of joint torques of the system, which is considered as the objective function with respect to linear equality and inequality constraints. Therefore, objective function is expressed as follows:

$$\text{Minimize } \Phi = \sum_{i=1}^{6} \sum_{j=1}^{3} M_{ij}^2(t) \tag{9}$$

subject to (a) inequality and (b) equality constraints (for details of the constraints, refer to [19]).

Here, $M_{ij}(t)$ is the joint torque variable and is a function of primary variables known as the foot force $\mathbf{F}_i$. Substituting the value of $M_{ij}(t)$ and rearranging, the Eq. (9), the objective function can be expressed in the standard form, as given below.

$$\text{Minimize } \Phi = \mathbf{x}^T \hat{\mathbf{H}} \mathbf{x} / 2 + \mathbf{C}^T \mathbf{x} \tag{10}$$

where $\hat{\mathbf{H}}$ is a hessian square matrix that includes the coefficients of all the quadratic terms; $\mathbf{C}$ is the column matrix that includes the coefficient of all the linear terms and $\mathbf{x}$ is the composite contact force vector of the objective function.

5 Simulations- Staircase Climbing Hexapod Robot

In the present study, at first, the kinematics of the system is analysed to determine the kinematic parameters. Thereafter, multibody dynamic analysis of the system is carried out with the motion inputs obtained from the kinematics study.

The position and orientation of the initial configuration of the robot are provided as inputs to the system. Here, the frame $\boldsymbol{G}_0$ and $\boldsymbol{G}$ are assumed to be parallel and they coincide at origin $\mathbf{O}$, that is, $\boldsymbol{\eta}_G = (0, 0, 0)^T$. Also, it is assumed that the robot's trunk body remains parallel to the slope of the staircase at any instant of time. Therefore, the value of angle α_0 is determined from the relationship , as given below.

$$\alpha_0 = \tan^{-1}(h_s / b_s) \tag{11}$$

Since the robot is assumed to be parallel to the slope at any instant of time during locomotion, the other angles that is, $\beta_0 = \theta_0 = 0$. Hence, at time $t=0$, the position and orientation of $\boldsymbol{P}_0$ with respect to global frame $\boldsymbol{G}$ are given by $\mathbf{p}_0^G = \{0, 0.412, 0.235, \tan^{-1}(h_s / b_s), 0, 0\}^T$. The corresponding initial joint angles are calculated from the CAD model. Also, it is assumed that there is no slippage between foot-tip and ground, as the robot climbs upstairs.

The kinematic analysis is carried out in MATLAB solver for three duty cycles with time step $h=0.05$. The total simulation time to execute the motion of the robot for three duty cycles is 8.6s (1st cycle- 3.0s, 2nd cycle- 2.6s, 3rd cycle- 3s). The calculated kinematic motion parameters (position, velocity and acceleration) of the tip point $\mathbf{P}_{i3}$ ($i=1$ to 6), based on the motion and gait planning algorithm (refer to [18]) are provided as inputs to the inverse dynamic analysis of the system. The MATLAB optimization solver chosen in the present case is *interior-point-convex*

quadprog algorithm that satisfies the boundary conditions at each iteration corresponding to the objective function. The torque is limited to ±6Nm.

The computed results of the force distribution in the legs, joint torques, power consumptions are plotted over three gait cycles with a total cycle time of 8.6s. Figure 3 shows the normal feet-force component F_{iz} of all the six legs of the hexapod plotted against time at an interval of h=0.05s. For a tripod wave-gait, the support and swing phase times are equal for all the legs following a sequence: 1) legs 1-4-5 in support phase and legs 2-3-6 in swing phase; 2) legs 2-3-6 in support phase and legs 1-4-5 in swing phase (refer to Fig. 1 for the leg numbering sequence).

A close observation of the Fig. 3(a) reveals that the pattern of the reaction foot force F_{iz} experienced by the legs 1-2, 3-4 and 5-6 are similar except that the pattern is out of phase by 180^0. This may be attributed to the fact that wave gaits are regular and symmetric, with the right and left legs of each column having a phase difference of a half-cycle. When the legs are lifted during swing phase, the forces on leg tips are zero and denoted by straight line. Further, it is observed that as the trunk body climbs upstairs with straight-forward motion, the entire center of gravity of the hexapod will move forward. Hence, feet forces on the front leg, which is in support phase, will increase while that on the rear leg will decrease with time till the start of swing phase. In addition to the above, it is also seen that the sum of all the feet forces along z-direction with respect to $\boldsymbol{G}_0$ balances the weight of the hexapod (65.7 N) at any instant of time (Fig.3a) except at the time of impact. A close view of the graph is shown in Fig. 3(b), from where one can infer that the when the leg tip collides with the terrain (start of support phase), a momentary impulsive force is generated.

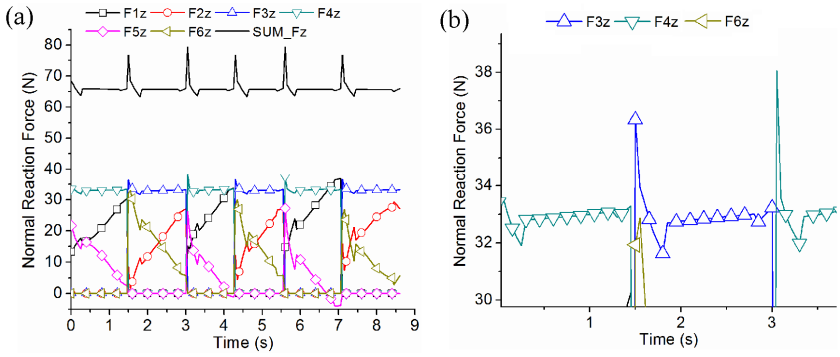

Figure 3: Normal Feet force distribution for duty factor DF=1/2 during staircase climbing (a) all legs with respect to frame $\boldsymbol{G}_0$ (b) Close view depicting the momentarily normal impact force for the legs 3 and 4.

Figure 4 shows the joint torques in legs 1 and 2. The torques in support phase take significant values, while in swing phase they are close to zero. Moreover, during the entire duration of climb, the torque distribution in joint 1 is minimum of the three joints for each leg. It is also observed that the joint 2 experiences maximum torque compared to the other joints at any instant of time. Further, the effect of the impulsive force can be well observed in the joint torque distribution of the legs. There are momentarily sharp changes (increase or decrease) in the values of torques. The variations of instantaneous power (P_{in}) consumption throughout a locomotive cycle of the hexapod are shown in Fig. 5. The highest peak arises at the time, when the swing and support legs change stance.

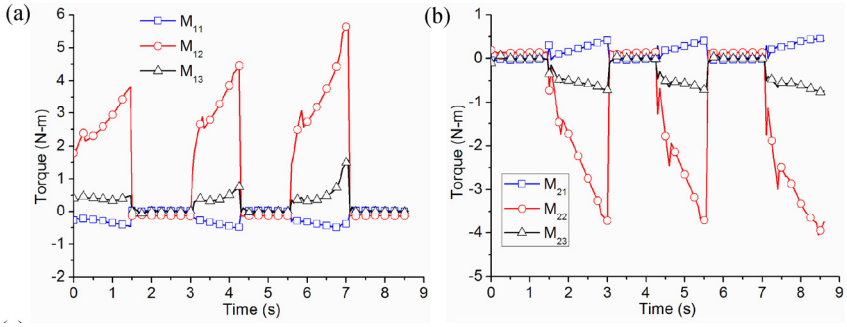

Figure 4: Joint Torque distribution for duty factor DF=1/2 during staircase climbing (a) Leg 1, (b) Leg2

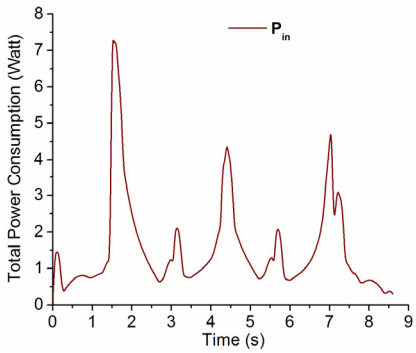

Figure 5: Instantaneous power consumption (P_{in}) of all the joints

6 Conclusions

The simulation results establish the impact-based feet-terrain interaction model without slippage or sliding of the feet-tip with respect to regular uneven terrain (like a staircase) for a constrained inverse dynamical system. Optimal feet-force distributions in the legs, corresponding to minimization of the sum of squares of joint torques are computed using quadratic programming. Momentary spikes are observed in the force versus time plot, which depicts the impulsive collision at the instant when the leg tip strikes the ground. Significant changes in the torque and overall power consumption are also observed during collision. The effects of impact and slip on energy efficiency with different gait patterns and walking speeds will be studied in the future.

References

[1] Q. Bombled and O. Verlinden, “Dynamic simulation of six-legged robots with a focus on joint friction”, Multibody Syst Dyn, Vol. 28(4), pp 395-417, 2012. DOI 10.1007/s11044-012-9305-z.

[2] Y. Zheng and W.-H. Qian, “Coping with the grasping uncertainities in force-closure analysis”, Int J of Rob Research, vol. 24 (4), pp. 311-327, 2004.

[3] W. Kwon and B. H. Lee, “A New Optimal Force Distribution Scheme of Multiple Cooperating Robots Using Dual Method”, J Intell Robot Syst, vol. 21(4), pp. 301–326, 1998.

[4] S. S. Roy , A. K.Singh and D. K.Pratihar, "Estimation of optimal feet forces and joint torques for on-line control of six-legged robot", Robotics and Computer-Intergrated Manufacturing, vol. 27(5), pp. 910–917, 2011.
[5] M. S. Erden and K. Leblebicioglu, "Torque distribution in a six-legged robot", IEEE Trans. On Robotics, vol. 23 (1), pp. 179-186, 2007.
[6] D. C. Kar, K. Kurien Issac and K. Jayarajan, "Minimum Energy Force Distribution for a Walking Robot", J of Rob Syst, vol.18(2), pp. 47-54, 2001.
[7] D.W. Marhefka, D.E. Orin, "A compliant contact model with nonlinear damping for simulation of robotic systems", IEEE Trans on Syst, Man and Cybernetics, Part A: Systems and Humans, vol. 29, pp. 566–572, 1999.
[8] T. Chanthasopeephan, A. Jarakorn, P. Polchankajorn, T. Maneewarn, "Impact reduction mobile robot and the design of the compliant legs, Robotics and Autonomous Systems", vol. 62(1), pp. 38–45, 2014.
[9] V. Vasilopoulos, I. S. Paraskevas and E. G. Papadopoulos, "Compliant terrain legged locomotion using a viscoplastic approach", IEEE/RSJ International Conference on Intelligent Robots and Systems (IROS 2014) , pp. 4849-4854
[10] K. Hunt and F. Crossley, "Coefficient of restitution interpreted as damping in vibroimpact", Trans. of the ASME- J. Appl. Mech., vol 42, pp. 440–445, 1975.
[11] Y. Xu, J. Yao and Y. Zhao, "Inverse dynamics and internal forces of the redundantly actuated parallel manipulators", Mech. and Machine Theory, vol. 51, pp. 172–184, 2012.
[12] H. Hemami, B. F. Wyman, "Rigid Body Dynamics, Constraints, and Inverses, Trans. of the ASME- Journal of Applied Mechanics, vol. 74, pp. 47-56, 2007.
[13] F. T. Cheng and D. E. Orin, "Efficient algorithm for optimal force distribution the Compact-Dual LP method", IEEE Trans. on Robotics and Automation, vol. 6 (2), pp. 178-187, 1990.
[14] J.-S. Chen, F.-T. Cheng, K.-T. Yang, F.-C. Kung and Y.-Y. Sun, "Optimal force distribution in multilegged vehicles", Robotica, vol. 17, pp. 159–172, 1999.
[15] M. S. Erden and K. Leblebicioglu, "Torque distribution in a six-legged robot", IEEE Trans. on Robotics, vol. 23 (1), pp. 179-186, 2007.
[16] S. S. Roy and D. K. Pratihar, "Kinematics, Dynamics and Power Consumption Analyses for Turning Motion of a Six-Legged Robot", J Intell Robot Syst, Vol. 74 (3-4), pp. 663-688, 2014. DOI: 10.1007/s10846-013-9850-6.
[17] V. Kumar and K. J. Waldron, "Gait analysis for walking machines for omnidirectional locomotion on uneven terrain", Proc. of 7th CISM-IFToMM Symp.- Theory and Practice of Robots and Manipulators, Edited by A. Morecki, G. bianchi and K. Kectzior, Udine, Italy, pp. 37-62, 1988.
[18] A. Mahapatra, S. S. Roy and D. K. Pratihar, Computer aided modeling and analysis of turning motion of hexapod robot on varying terrains, Int J of Mechanics and Materials in Design, 2015. DOI:10.1007/s10999-015-9315-0
[19] A. Mahapatra, K. Bhavanibhatla, S.S. Roy and Pratihar D.K., "Energy-efficient inverse dynamic model of a hexapod robot", Proc. of the IEEE Int. Conf. on Robotics, Automation, Control and Embedded Systems, (RACE2015), Chennai, India, pp. 1-7, 2015. DOI:10.1109/RACE.2015.7097237.